Supplementary Information

for

Development and performances analysis of eco-friendly Pullulan/ Polyvinyl Alcohol composites based all-solid state supercapacitors

Elyes Bel Hadj Jrad[a,c], Francesca Soavi[b*], and Chérif Dridi[a*]

[a]NANOMISENE Laboratory LR16CRMN01, Center for Research in Microelectronics and Nanotechnology of Sousse, Sahloul Sousse 4054, Tunisia
[b]Department of Chemistry "Giacomo Ciamician", Laboratory of Electrochemistry of Material for Energetics, Alma Mater Studiorum, Universita' di Bologna, Italy

[c]Higher School of Science and Technology of Hammam Sousse, Hammam Sousse 4011, Tunisia
*Corresponding authors
francesca.soavi@unibo.it

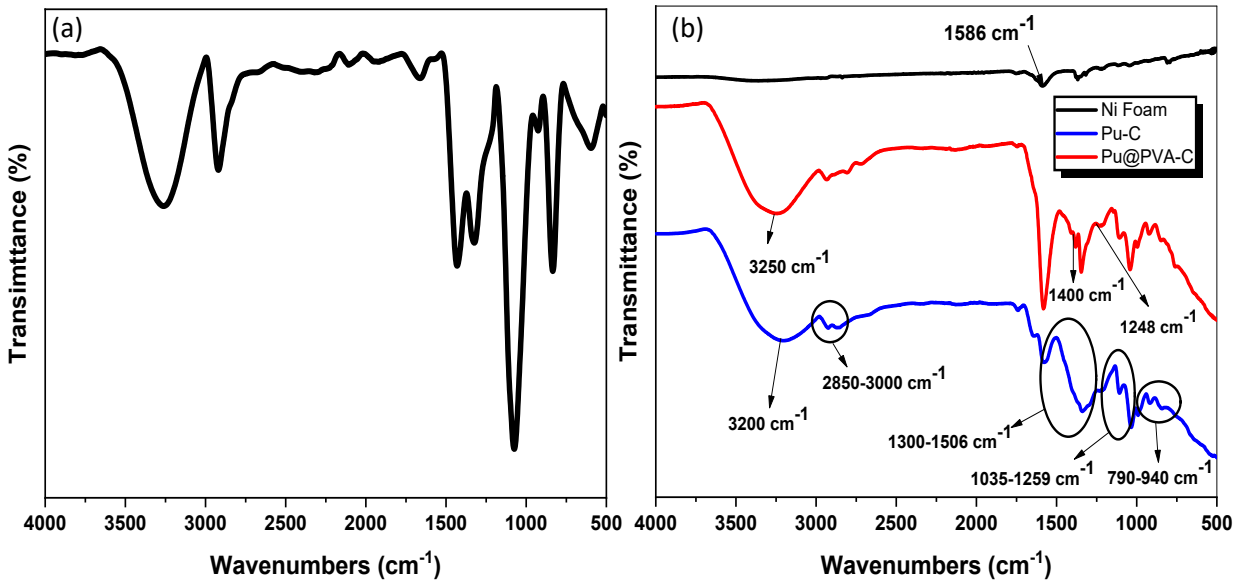

Fig. S1 (a) IR spectrum of (a) Pure PVA from ref . [1], (b) Nickel foam, Pu-C and Pu@PVA-C films respectively.

I.A. Plugariu and co-authors [2] worked Poly(vinyl alcohol)/Pullulan Composite Hydrogels and investigated the morphological, viscoelastic properties as well as the swelling behavior of such composites. They proved that the intermolecular interactions

act as physical crosslinking points, leading to the formation of a 3D network structure. The composite formation is mainly governed by hydrogen bonding among the −OH groups of PVA chains, as well as between PVA and Pullulan macromolecules.

Moreover, it is worth noting that the FTIR spectrum of PVA/Pullulan is well established and reported in M.R. Karim et al. work [3], where the broad O–H stretching band in the 3000–3600 cm^{-1} region is reported without significant variation. Yet, the authors demonstrated that with the addition of PVA, some absorption peaks of Pullulan become lower in intensity, whereas some others decrease with augmenting the concentration of PVA. Also, some additional peaks appear according to the same reference, which is consistent with fig S1(b) above. Still, the authors showed that both spectra (of bare pullulan and pullulan/PVA) share the same features with slight decrease in intensity for the band in the 3000–3600 cm^{-1} region upon the addition of PVA to 40% which could confirm restricted vibrations of the functional groups due to hydrogen bonding interactions.

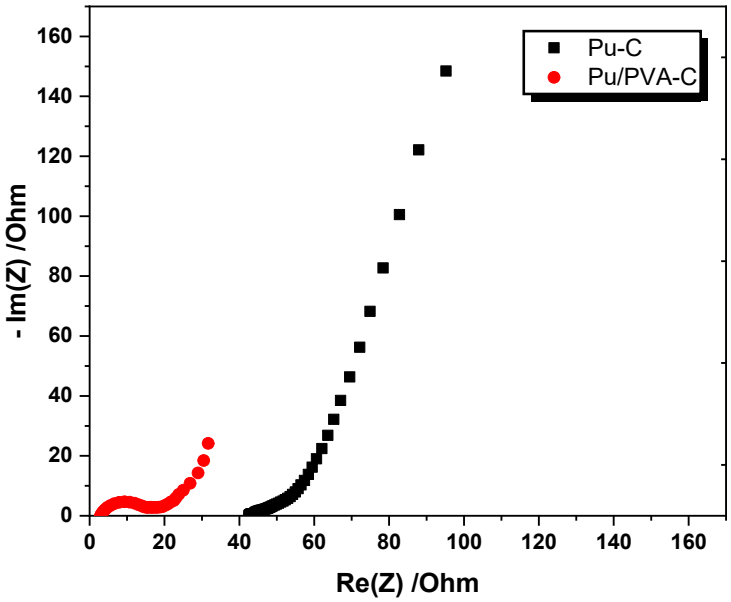

Fig. S2 Nyquist plots for Pu-C and Pu/PVA-C electrodes, respectively from 100 kHz to 100 mHz.

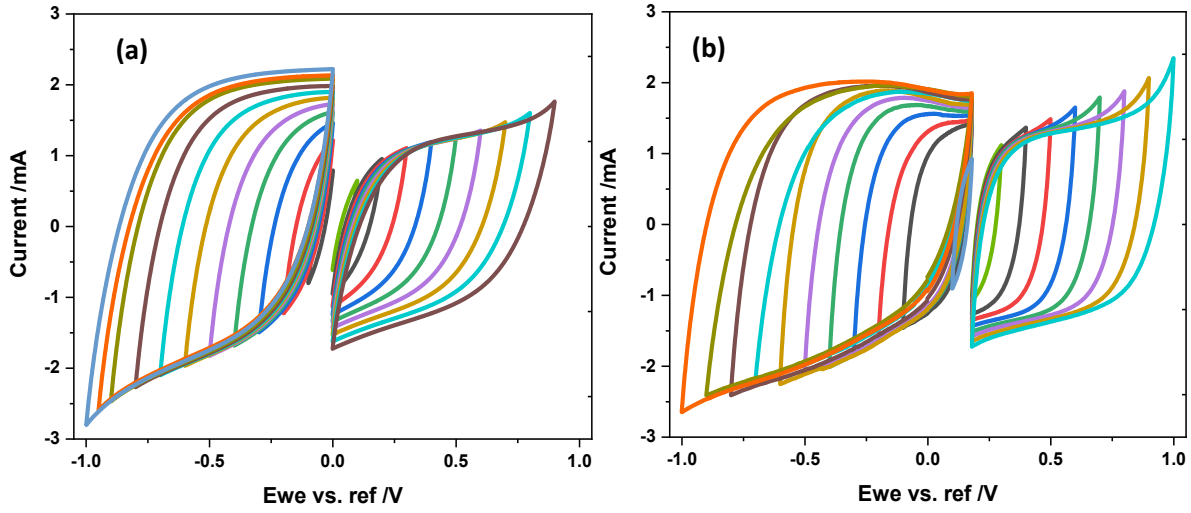

Fig. S3 CV plots of **(a)** Pu-C and **(b)** Pu/PVA-C respectively from -1 to 1 V at 20 mVs^{-1}.

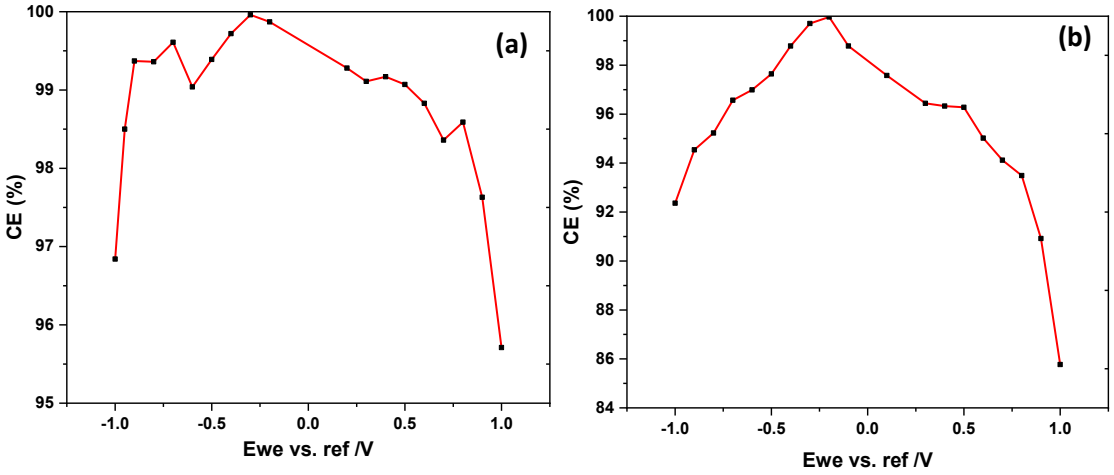

Fig. S4 CE variations as a function of potential, of **(a)** Pu-C and **(b)** Pu/PVA-C respectively.

Currently, there is no definitive standard or criterion for determining the most suitable equivalent electrical circuit from the simulation data. Therefore, the selection of the equivalent electrical circuit for this study was guided by the Root Mean Square Error (RMSE) criterion. The proposed electrical models (listed in table S1) were applied for the Pu-PVA-D Nyquist plots. Errors between the experimental data and the theoretical predictions were evaluated using the equation as follows. All errors calculations were performed under the same conditions using Levenberg-Marquardt method, over 5000 iterations, through ZFit fitting tool.

$$RMSE = \sqrt{\frac{\sum (P_i - O_i)^2}{n}} \qquad \textbf{(1)}$$

Where Pi and Oi are the predicted and observed values for the observations respectively, and n is the number of captured data. This method allowed us to identify which model resulted in the lowest RMSE values, which directly indicates the accuracy levels in the model's predictions. The smaller the RMSE, the closer the predicted values are to the actual values. According to the table, the model proposed in this study, along with those developed by D. B. Dubal [4], exhibits RMSE values that are closer to zero, indicating superior accuracy compared to the other mentioned models.

Table S1 Different equivalent electrical circuits adopted for single cell configurations for Nyquist plots modeling.

Electrode's composition	EIS parameters	Equivalent Electrical Circuit	RMSE	Refs.
rGO-Phosphotungstate	-	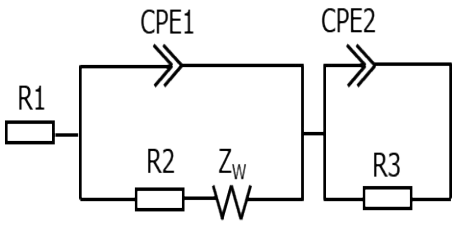	0.81	[4]
Carbon Ink	1 MHz-1Hz 10 mV	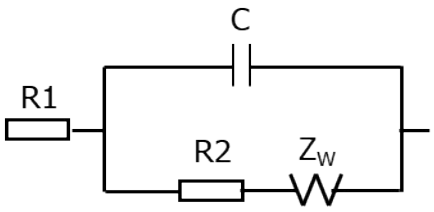	4.76	[5]
Activated Carbon	-	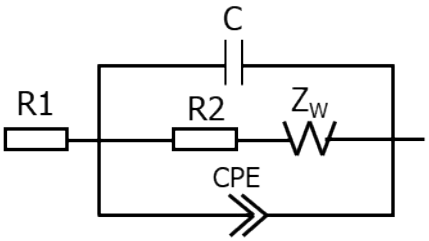	4.98	[6]
Activated Carbon Fibers	100 kHz-10 mHz 10 mV	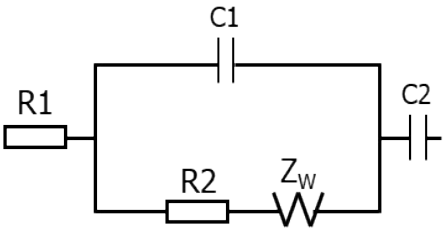	1.53	[7]
Commercial Activated Carbon	100 kHz – 100 mHz 10 mV	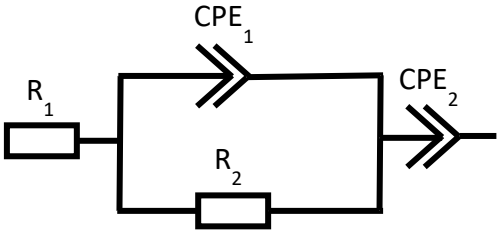	0.83	**This work, Ref.** [1]

The equivalent circuit showed in the last row of table S1 is the one adopted in this study. R_1 is related to the electronic contact resistance, and electrolyte ionic resistance. R_2 refers to percolation resistances (electronic resistance and ions resistance within the pores). The Constant Phase Element (CPE) is used to model the non-ideal capacitive behavior of a supercapacitor, and is expressed according to the following equation.

$$Z_{CPE} = \frac{1}{Q(j\omega)^n}$$

Where, Q is the CPE coefficient, $\omega = 2\pi f$ is the angular frequency, j is the imaginary unit and n is the phase exponent (0≤n≤1). The CPE exponent n quantifies the deviation from ideal capacitive behavior, with values closer to 1 indicating a more homogeneous and ideal electrode–electrolyte interface, and lower values reflecting increased surface roughness,

heterogeneity, and distributed ion-transport processes. In this work, CPE_1 refers to the capacitance associated with the electrode's external surface, whereas CPE_2 is related the diffusion limited process at the low frequency region.

Table S2. Maximum cell voltage (ΔV), discharge time (ΔV), areal and specific capacitance, power and energy performance for Pu-D and Pu/PVA-D supercapacitors at 0.5 A/g.

	ΔV (V)	Δt (s)	C ($mF.cm^{-2}$)	P ($mW.cm^{-2}$)	E ($\mu Wh.cm^{-2}$)	CE (%)
Pu-D	0.15	26.18	75 (19 F/g)	2.82	20.36	96.62
Pu/PVA-D	0.14	28.28	92 (23 F/g)	3.19	24.94	91.77

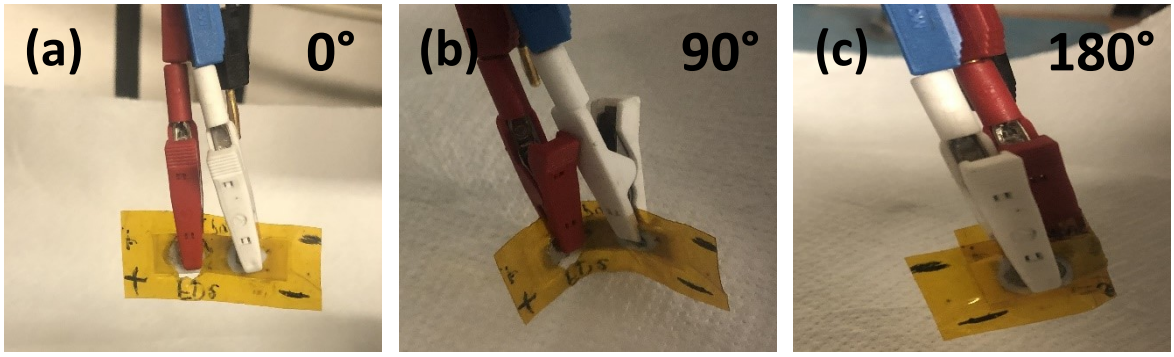

Fig. S5 Pu/PVA-C based supercapacitors folded at different bending angles (a) 0° (b) 90° and (c) 180° respectively.

References

1 E. Bel Hadj Jrad, F. Soavi and C. Dridi, *J. Energy Storage*, 2024, **88**, 111471.
2 I.-A. Plugariu, M. Bercea, L. M. Gradinaru, D. Rusu and A. Lupu, *Gels*, 2023, **9**, 580.
3 M. R. Karim and Md. S. Islam, *J. Nanomater.*, 2011, **2011**, 1–7.
4 D. P. Dubal, B. Nagar, J. Suarez-Guevara, D. Tonti, E. Enciso, P. Palomino and P. Gomez-Romero, *Mater. Today Energy*, 2017, **5**, 58–65.
5 C. Rokaya, J. Keskinen and D. Lupo, *J. Energy Storage*, 2022, **50**, 104221.
6 N. I. Muthi Aturroifah, M. Diantoro, W. Meevasana and S. Maensiri, *E3S Web Conf.*, 2024, **517**, 10003.
7 V. M. Igba, M. A. Garcia-Lobato, U. M. García-Pérez, E. Oyervides-Muñoz and E. I. Martínez-Mora, *Ionics*, DOI:10.1007/s11581-024-05701-3.